Reactions of a Hexahydride−Osmium Complex with Aromatic Ketones: C−H Activation versus C−F Activation§

Pilar Barrio,† Ricardo Castarlenas,† Miguel A. Esteruelas,*,† Agustí Lledós,*,‡ Feliu Maseras,‡ Enrique Oñate,† and Jaume Tomàs‡

Departamento de Química Inorgánica, Instituto de Ciencia de Materiales de Aragón, Universidad de Zaragoza-CSIC, 50009 Zaragoza, Spain, and Unitat de Química Física, Departament de Química, Universitat Autònoma de Barcelona, 08193 Bellaterra, Barcelona, Spain

Received October 3, 2000

Treatment of $OsH_6(P^iPr_3)_2$ (**1**) with benzophenone and acetophenone in toluene under reflux affords $OsH_3\{C_6H_4C(O)R\}(P^iPr_3)_2$ (R = Ph (**2**), CH_3 (**3**)), as a result of the *ortho*-CH activation of the aromatic group of the ketones. Complex **1** is also capable of activating *ortho*-CF bonds of fluorinated aromatic ketones. Thus, the reactions of this complex with pentafluoroacetophenone, decafluorobenzophenone, and 2,6-difluoroacetophenone give $OsH_3\{C_6F_4C(O)R\}(PiPr_3)_2$ (R = CH_3 (**4**), C_6F_5 (**5**)) and $OsH_3\{C_6H_3FC(O)CH_3\}(P^iPr_3)_2$ (**6**). The structure of **4** has been determined by X-ray diffraction. The geometry around the osmium atom can be described as a distorted pentagonal bipyramid with the phosphine ligands occupying axial positions. Complexes **4** and **6** can be also obtained by reaction of **1** with 2,3,4,5-tetrafluoroacetophenone and 2-fluoroacetophenone, respectively. This selective C−H activation of the *ortho*-CH bond of the above-mentioned ketones is in contrast with the selective C−F activation observed for the reaction of **1** with 2,3,4,5,6-pentafluorobenzophenone, which affords $OsH_3\{C_6F_4C(O)C_6H_5\}(P^iPr_3)_2$ (**7**). The structure of **7** has also been determined by X-ray diffraction. The geometry around the osmium is the same as that of **4**. DFT calculations suggest that in fluorinated aromatic ketones the *ortho*-CF activation is thermodynamically favored over the *ortho*-CH activation and that the kinetically preferred *ortho*-CH activation of 2,3,4,5-tetrafluoroacetophenone and 2-fluoroacetophenone is in part due to the preferred *anti* arrangement of the *F−C−*C−*C*═*O* unit of the starting ketones. In solution, the hydride ligands of the OsH_3 unit of **2**−**7** undergo two different thermally activated exchange processes, which involve the central hydride with each hydride ligand situated close to the donor atoms of the chelate group. The exchange involving the hydride ligand disposed *cis* to the carbonyl group is faster than the other one in all the cases. For **2**, **3**, and **6**, quantum exchange coupling is also observed between the hydride ligands involved in the faster thermally activated exchange process.

Introduction

The activation of C−H bonds by transition metal compounds has attracted a great deal of attention in recent years,[1] in particular the selectivity of the competitive alkane−arene intermolecular activation.[2] Although the arene C−H bond is between 8 and 14 kcal·mol^{-1} stronger than the alkane C−H bond, in general, the activation of the first one is kinetically and thermodynamically favored. The kinetic advantage of the arene activation appears to be due to its prior π-coordination, while the thermodinamic preference has been largely attributed to a metal−carbon bond much stronger for aryl than for alkyl.

Activation of C−F bonds provides a chemical challenge akin to that of C−H activation in analogous hydrocarbon compounds.[3] Even though the C−F bonds are about 30 kcal·mol^{-1} stronger than the C−H bonds, in the past decade, a number of transition metal compounds, with the metal in low oxidation state, have shown to be capable of the intermolecular activation of aromatic C−F bonds,[4] including catalysis.[5]

The broadly used substrate has been hexafluorobenzene. The first record of this type of activation involved

§ Dedicated to Professor Rafael Usón on the occasion of his 75th birthday.

† Universidad de Zaragoza-CSIC.

‡ Universitat Autònoma de Barcelona.

(1) (a) Shilov, A. E. *Activation of Saturated Hydrocarbons by Transition Metal Complexes*; D. Riedel Publising Co.: Dordrecht, The Netherlands, 1984. (b) Bergman, R. G. *Science* **1984**, *223*, 902. (c) Halpern, J. *Inorg. Chim. Acta* **1985**, *100*, 41. (d) Crabtree, R. H. *Chem. Rev.* **1985**, *85*, 245. (e) Grenn, M. L. H.; O'Hare, D. *Pure Appl. Chem.* **1985**, *57*, 1897. (f) *Activation and Functionalization of Alkenes*; Hill, C. L., Ed.; John Wiley and Sons: New York, 1989; Chapter IV, p 11. (g) Ryabov, A. D. *Chem. Rev.* **1990**, *90*, 403. (h) Arndtsen, B. A.; Bergman, R. G.; Mobley, T. A.; Peterson, T. H. *Acc. Chem. Res.* **1995**, *28*, 154. (i) Sen, A. *Acc. Chem. Res.* **1998**, *31*, 550.

(2) Jones, W. D.; Feher, F. J. *Acc. Chem. Res.* **1989**, *22*, 91.

10.1021/om000844r CCC: $20.00
Publication on Web 01/03/2001

oxidative addition at $Ni(PEt_3)_2$ to yield *trans*-$Ni(C_6F_5)(F)(PEt_3)_2$.[6] Related nickel and platinum complexes with chelating ligands also undergo oxidative addition with hexafluorobenzene.[7] Reaction of hexafluorobenzene with $Ir(CH_3)(PEt_3)_3$ results in a unique process involving C−F bond cleavage, P−C bond cleavage, and P−F bond formation, affording *trans*-$Ir(C_6F_5)(PFEt_2)(PEt_3)_2$.[8] Another successful approach has been the photolysis of $Re(\eta^5\text{-}C_5Me_5)(CO)_3$ in hexafluorobenzene at room temperature, which gives $Re(\eta^5\text{-}C_5Me_4CH_2)(C_6F_5)(CO)_2$ formed by insertion into a C−F bond of C_6F_6 and concomitant insertion into a methyl C−H bond.[9] Jones, Perutz, and co-workers have also studied the photochemically promoted C−F bond cleavage with $Rh(\eta^5\text{-}C_5Me_5)(\eta^2\text{-}C_2H_4)(PMe_3)$ and $IrH_2(\eta^5\text{-}C_5H_5)(PMe_3)$.[10] Irradiation of $Rh(\eta^5\text{-}C_5Me_5)(\eta^2\text{-}C_2H_4)(PMe_3)$ in hexafluorobenzene leads to the initial formation of $Rh(\eta^5\text{-}C_5Me_5)(\eta^2\text{-}C_6F_6)(PMe_3)$, and continued photolysis affords $Rh(\eta^5\text{-}C_5Me_5)(C_6F_5)(F)(PMe_3)$. Photolysis of $IrH_2(\eta^5\text{-}C_5H_5)(PMe_3)$ in hexafluorobenzene generates $Ir(\eta^5\text{-}C_5H_5)(C_6F_5)(F)(PMe_3)$ and $Ir(\eta^5\text{-}C_5H_5)(\eta^2\text{-}C_6F_6)(PMe_3)$. Recently, Jones and co-workers have observed that the complex $RhH_2(\eta^5\text{-}C_5Me_5)(PMe_3)$ reacts with polyfluorinated arenes in pyridine to give the C−F cleavage products $RhH(\eta^5\text{-}C_5Me_5)(aryl^F)(PMe_3)$ in high yield.[11]

The selectivity of the C−F versus C−H activation has received scarce attention, and the trend is not clear. The reactivity of partially fluorinated arenes $C_6F_nH_{6-n}$ ($n = 1-5$) depends on the nature of the transition metal system. The thermally generated fragment $Rh(\eta^5\text{-}C_5Me_5)(PMe_3)$ and the photochemically generated fragment $Rh(\eta^5\text{-}C_5H_5)(PMe_3)$ both react with partially fluorinated arenes to yield C−H activation products.[12] Similar results have been obtained with the osmium complex $OsH(C_6H_5)(CO)(P^tBu_2Me)_2$.[13] However, *cis*-$RuH_2(dmpe)_2$ is selective for C−F over C−H activation.[14]

In 1993, Murai and co-workers reported that the C−H bond at the *ortho* position of aromatic ketones selectively adds to the double bond of olefins using the ruthenium complex $RuH_2(CO)(PPh_3)_3$ as catalyst.[15] Murai's reaction is now one of the most important processes in organic synthesis, which allows not only the alkylation of aromatic ketones[16] but also the alkylation of aromatic esters[17] and imines[18] and the copolymerization of aromatic ketones and α,ω-divinylsilanes.[19] The reactions involve the coordination of the carbonyl group to the ruthenium atom of the catalyst, followed by the C−H activation of the *ortho*-CH bond of the aromatic ring. The coordination of the carbonyl oxygen atom is considered to be the origin of the high *ortho* selectivity.[20] Experimental evidence suggests that the olefin is initially hydrogenated to give the d^8 derivative $Ru(CO)(PPh_3)_3$, which has been proposed to be a candidate of the active species.[16,21] Recently, Chaudret and co-workers have observed that $RuH_2(\eta^2\text{-}H_2)_2(PR_3)_2$ can also act as catalyst precursor.[22]

Although, in the past few years, a number of interesting examples of organic transformations catalyzed by osmium complexes have emerged,[23] it is also true that traditionally some of them have served as stable models of reactive intermediates, proposed in catalytic transformations with the ruthenium counterparts. This, along with our interest to know whether aromatic ketones, totally and partially fluorinated, could be alkylated by the Murai's method, and the requirement of the ketone to keep the fluoride atom in the *ortho* position, prompted us to study the reactivity of the

(3) (a) Bruce, M. I.; Goodall, B. L.; Sheppard, G. L.; Stone, F. G. A. *J. Chem. Soc., Dalton Trans.* **1975**, 591. (b) Bruce, M. I.; Gardner, R. C. F.; Stone, F. G. A. *J. Chem. Soc., Dalton Trans.* **1976**, 81. (c) MacNicol, D. D.; Robertson, C. D. *Nature* **1988**, *332*, 59. (d) Anderson, C. M.; Crespo, M.; Ferguson, G.; Lough, A. J.; Puddephatt, R. J. *Organometallics* **1992**, *11*, 1177. (e) Crespo M.; Martínez, M.; Sales, J. *Organometallics* **1993**, *12*, 4297. (f) Vicente, J.; Chicote, M. T.; Fernández-Baeza, J.; Fernández-Baeza, A.; Jones, P. G. *J. Am. Chem. Soc.* **1993**, *115*, 794. (g) Harrison, R. G.; Richmond, T. G. *J. Am. Chem. Soc.* **1993**, *115*, 5303. (h) Samuels, J. A.; Lobkovsky, E. B.; Streib, W. E.; Folting, K.; Huffman, J. C.; Zwanziger, J. W.; Caulton, K. G. *J. Am. Chem. Soc.* **1993**, *115*, 5093. (i) Weydert, M.; Andersen, R. A.; Bergman, R. G. *J. Am. Chem. Soc.* **1993**, *115*, 8837. (j) Kiplinger, J. L.; Richmond, T. G.; Ostemberg, C. E. *Chem. Rev.* **1994**, *94*, 373. (k) Vicente, J.; Chicote, M. T.; Fernández-Baeza, J.; Fernández-Baeza, A. *New J. Chem.* **1994**, *18*, 263. (l) Bennett, B. K.; Harrison, R. G.; Richmond, T. G. *J. Am. Chem. Soc.* **1994**, *116*, 11165. (m) Falvello, L. R.; Forniés, J.; Navarro, R,; Rueda, A.; Urriolabeitia, E. P. *Organometallics* **1996**, *15*, 309. (n) Kiplinger, J. L.; Richmond T. G. *J. Am. Chem. Soc.* **1996**, *118*, 1805. (o) Su, M.-D.; Chu, S.-Y. *J. Am. Chem. Soc.* **1997**, *119*, 10178. (p) Hughes, R. P.; Lindner, D. C.; Rheingold, A. L.; Liable-Sands, L. M. *J. Am. Chem. Soc.* **1997**, *119*, 11544. (q) Lopez, O.; Crespo, M.; Font-Bardía, M.; Solans, X. *Organometallics* **1997**, *16*, 1233. (r) Hughes, R. P.; Smith, J. M. *J. Am. Chem. Soc.* **1999**, *121*, 6084. (s) Yang, H.; Gao, H.; Angelici, R. J. *Organometallics* **1999**, *18*, 2285. (t) Godoy, F.; Higgitt, C. L.; Klahn, A. H.; Oelckers, B.; Parsons, S.; Perutz, R. N. *J. Chem. Soc., Dalton Trans.* **1999**, 2039. (u) Guennou-de Cadenet, K.; Rumin, R.; Pétillon, F. Y. *Organometallics* **2000**, *19*, 1912.

(4) Burdeniuc, J.; Jedlicka, B.; Crabtree, R. H. *Chem. Ber.* **1997**, *130*, 145.

(5) (a) Aizenberg, M.; Milstein, D. *Science* **1994**, *265*, 359. (b) Aizenberg, M.; Milstein, D. *J. Am. Chem. Soc.* **1995**, *117*, 8674.

(6) (a) Fahey, D. R.; Mahan, J. E. *J. Am. Chem. Soc.* **1977**, *99*, 2501. (b) Cronin, L.; Higgitt, C. L.; Karch, R.; Perutz, R. N. *Organometallics* **1997**, *16*, 4920.

(7) (a) Hofmann, P.; Unfried, G. *Chem. Ber.* **1992**, *125*, 659. (b) Bach, I.; Pörschke, K.-R.; Goddard, R.; Kopiske, C.; Krüger, C.; Rufin'ska, A.; Seevogel, K. *Organometallics* **1996**, *15*, 4959. (c) Yamamoto, T.; Abla, M. *J. Organomet. Chem.* **1997**, *535*, 209.

(8) Blum, O.; Frolow, F.; Milstein, D. *J. Chem. Soc., Chem. Commun.* **1991**, 258.

(9) Klahn, A. H.; Moore, M. H.; Perutz, R. N. *J. Chem. Soc., Chem. Commun.* **1992**, 1699.

(10) (a) Jones, W. D.; Partridge, M. G.; Perutz, R. N. *J. Chem. Soc., Chem. Commun.* **1991**, 264. (b) Belt, S. T.; Helliwell, M.; Jones, W. D.; Partridge, M. G.; Perutz, R. N. *J. Am. Chem. Soc.* **1993**, *115*, 1429.

(11) Edelbach, B. L.; Jones, W. D. *J. Am. Chem. Soc.* **1997**, *119*, 7734.

(12) Selmeczy, A. D.; Jones, W. D.; Partridge, M. G.; Perutz, R. N. *Organometallics* **1994**, *13*, 522.

(13) Bosque, R.; Clot, E.; Fantacci, S.; Maseras, F.; Eisenstein, O.; Perutz, R. N.; Renkema, K. B.; Caulton, K. G. *J. Am. Chem. Soc.* **1998**, *120*, 12634.

(14) Whittlesey, M. K.; Perutz, R. N.; Moore, M. H. *J. Chem. Soc., Chem. Commun.* **1996**, 787.

(15) Murai, S.; Kakiuchi, F.; Sekine, S.; Tanaka, Y.; Kamatani, A.; Sonoda, M.; Chatani, N. *Nature* **1993**, *366*, 529.

(16) (a) Kakiuchi, F.; Sekine, S.; Tanaka, Y.; Kamatani, A.; Sonoda, M.; Chatani, N.; Murai. S. *Bull. Chem. Soc. Jpn.* **1995**, *68*, 62. (b) Murai, S.; Chatani, N.; Kakiuchi, F. *Pure Appl. Chem.* **1997**, *69*, 589.

(17) Sonoda, M.; Kakinchi, F.; Kamatani, A.; Chatani, N.; Murai, S. *Chem. Lett.* **1996**, 109.

(18) Kakiuchi, F.; Yamauchi, M.; Chatani, N.; Murai, S. *Chem. Lett.* **1996**, 111.

(19) (a) Guo, H.; Weber, W. P. *Polym. Bull.* **1994**, *32*, 525. (b) Tapsak, M. A.; Guo, H.; Weber, W. P. *Polym. Bull.* **1995**, *34*, 49. (c) Guo, H.; Wang, G.; Tapsak, M. A.; Weber, W. P. *Macromolecules* **1995**, *28*, 5686.

(20) (a) Matsubara, T.; Koga, N.; Musaev, D. G.; Morokuma, K. *J. Am. Chem. Soc.* **1998**, *120*, 12692. (b) Matsubara, T.; Koga, N.; Musaev, D. G.; Morokuma, K. *Organometallics* **2000**, *19*, 2318.

(21) Colombo, M.; George, M. W.; Moore, J. N.; Pattison, D. I.; Perutz, R. N.; Virrels, I. G.; Ye, T.-Q. J. *Chem. Soc., Dalton Trans.* **1997**, 2857.

(22) Guari, Y.; Sabo-Etienne, S.; Chaudret, B. *J. Am. Chem. Soc.* **1998**, *120*, 4228.

(23) (a) Chaloner, P. A.; Esteruelas, M. A.; Joó,F.; Oro, L. A. *Homogeneous Hydrogenation*; Kluwer Academic Publishers: Dordrecht, 1994. (b) Sánchez-Delgado, R. A.; Rosales, M.; Esteruelas, M. A.; Oro, L. A. *J. Mol. Catal. A: Chem.* **1995**, *96*, 231. (c) Esteruelas, M. A.; Oro, L. A. *Chem. Rev.* **1998**, *98*, 577.

hexahydride−osmium complex $OsH_6(P^iPr_3)_2$ toward aromatic ketones, partially fluorinated aromatic ketones, and totally fluorinated aromatic ketones. In this paper, we report the results of this study.

Results and Discussion

1. C−H Activation of Aromatic Ketones. Treatment under reflux of toluene solutions of the hexahydride complex $OsH_6(P^iPr_3)_2$ (**1**) with 1.2 equiv of benzophenone and acetophenone affords after 5 h dark solutions, from which the trihydride compounds $OsH_3\{C_6H_4C(O)R\}(P^iPr_3)_2$ (R = Ph (**2**), CH_3 (**3**)) were isolated in about 60% yield (eq 1).

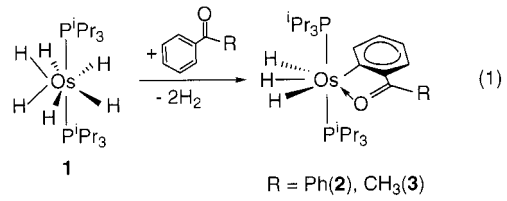

(1)

The spectroscopic data of **2** and **3** agree well with the structure proposed in eq 1. The IR spectra in KBr show ν(CO) vibrations at 1580 (**2**) and 1698 (**3**) cm^{-1}, along with three bands at 1946, 2133, and 2185 (**2**) and 1974, 2149, and 2170 (**3**) cm^{-1}, corresponding to the hydride ligands. In the $^{13}C\{^1H\}$ NMR spectra, the resonance due to the metalated carbon atoms of the ketones appear at 215.4 (**2**) and 211.4 (**3**) ppm as triplets with C−P coupling constants of about 6 Hz. In agreement with the mutually *trans* disposition of the phosphine ligands, the $^{31}P\{^1H\}$ NMR spectra in toluene-d_8 contain singlets at 31.3 (**2**) and 30.4 (**2**) ppm, which are temperature invariant between 370 and 180 K.

In contrast with the $^{31}P\{^1H\}$ NMR spectra, the ^1H NMR spectra are temperature-dependent. At 368 K, the spectrum of **2** shows in the hydride region a single resonance. This observation is consistent with the operation of two thermally activated exchange processes, which proceed at rates sufficient to lead to the single hydride resonance. Consistent with this, lowering the sample temperature leads to broadening of the resonance. At 293 K, the first decoalescence occurs, and at 233 K, the second one takes place. At this temperature, and $ABCX_2$ spin system (X = ^{31}P) is observed, which becomes well resolved at 223 K. The $^1H\{^{31}P\}$ spectra (Figure 1) are simplified to the expected ABC spin system. At 223 K, this spin system is defined by $\delta_A = -3.35$, $\delta_B = -11.13$, $\delta_C = -12.23$, $J_{AB} = 43.2$ Hz, and $J_{AC} = J_{BC} = 0$ Hz. Between 223 and 183 K, the values of the chemical shifts of A, B, and C sites, as well as that of J_{AC} and J_{BC}, show no significant temperature dependence. However, the magnitude of the observed J_{AB} is sensitive to the temperature, decreasing from 43.2 to 28.8 Hz as the temperature decreases from 233 to 183 K. This can be readily explained in terms of the quantum exchange coupling between H_A and H_B.[24]

The T_1 values of the hydrogen nuclei of the OsH_3 unit of **2** were determined over the temperature range 293−193 K. T_1(min) values of 69 ± 6 ms for H_A, 83 ± 3 ms for H_B, and 107 ± 1 for H_C were obtained at 228 K. They support the trihydride character of **2** and suggest that the central atom of the OsH_3 unit is H_A. To assign the positions of H_B and H_C, we carried out a ROESY ^1H NMR experiment at 213 K. This experiment (Figure 2) indicates that H_C is the hydride ligand located *cis* to

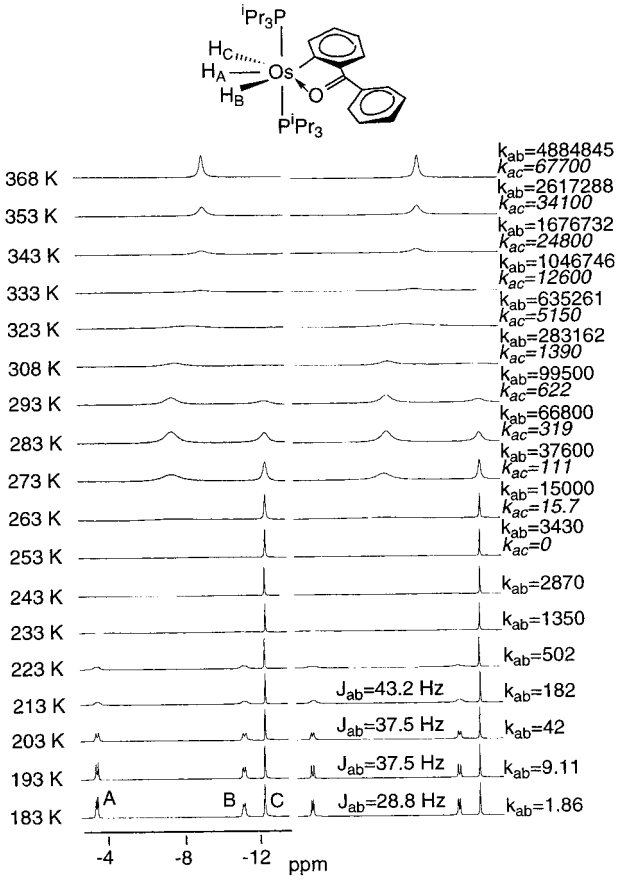

Figure 1. Left: Variable-temperature $^1H\{^{31}P\}$ NMR spectra (300 MHz) in C_7D_8 in the high-field region of $OsH_3\{C_6H_4C(O)C_6H_5\}(P^iPr_3)_2$ (**2**). Right: Simulated spectra, J_{AB}, temperatures and rate constants (s^{-1}) for the intramolecular hydrogen site-exchange process are also provided.

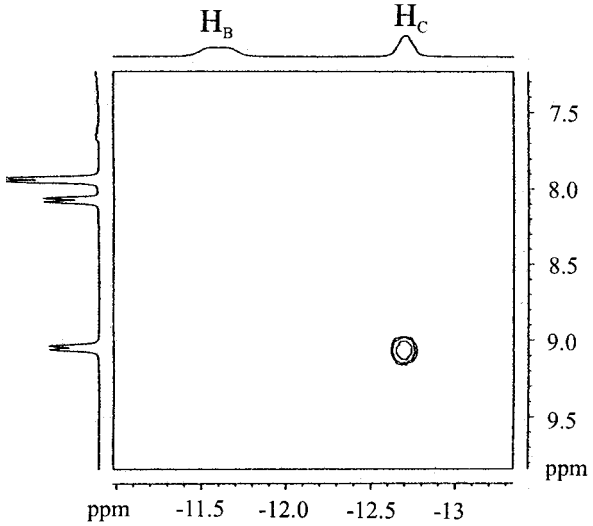

Figure 2. Partial view of the ROESY ^1H NMR spectrum at 213 K in C_7D_8 of $OsH_3\{C_6H_4C(O)C_6H_5\}(P^iPr_3)_2$ (**2**).

(24) Sabo-Etienne, S.; Chaudret, B. *Chem. Rev.* **1998**, *98*, 2077.

the metalated aromatic ring. So, H_B is the hydride situated *cis* to the carbonyl group.

Line shape analysis of the spectra of Figure 1 allows the calculation of the rate constants for the thermal exchange processes at different temperatures. The activation parameters obtained from the corresponding Eyring analysis are $\Delta H^{\ddagger} = 10.0 \pm 0.2$ kcal·mol^{-1} and $\Delta S^{\ddagger} = -1.1 \pm 0.4$ cal·mol^{-1}·K^{-1} for the H_A/H_B exchange and $\Delta H^{\ddagger} = 14.0 \pm 0.4$ kcal·mol^{-1} and $\Delta S^{\ddagger} = -1.8 \pm 0.8$ cal·mol^{-1}·K^{-1} for the H_A/H_C exchange. The values for the entropy of activation, close to zero, are in agreement with an intramolecular process, whereas the values for the enthalpy of activation lie in the range reported for thermal exchange processes in related osmium−trihydride complexes.[25]

The behavior of the hydrides of **3** with the temperature is the same as that found for **2**. The OsH_3 unit undergoes two thermal activated exchange processes. The activation parameters for the exchange involving the central hydride ($\delta = -4.09$) and the one disposed *cis* to the carbonyl group of the ketone ($\delta = -12.32$) are $\Delta H^{\ddagger} = 9.7 \pm 0.2$ kcal·mol^{-1} and $\Delta S^{\ddagger} = -3.8 \pm 0.5$ cal·mol^{-1}·K^{-1}, whereas the activation parameters for the exchange involving the central hydride and that disposed *cis* to the metalated phenyl ring ($\delta = -13.35$) are $\Delta H^{\ddagger} = 13.9 \pm 0.3$ kcal·mol^{-1} and $\Delta S^{\ddagger} = 0.83 \pm 0.7$ cal·mol^{-1}·K^{-1}. The central hydride and that disposed *cis* to the carbonyl group of the ketone also undergo quantum exchange coupling with a decrease of the H−H coupling constant from 39.0 to 19.5 Hz as the temperature decreases from 213 to 183 K.

The reaction shown in eq 1 indicates that the activation of aromatic ketones occurs not only with metallic centers in low oxidation states but also with those in high oxidation states. The formation of **2** and **3** would involve the thermal activation of $OsH_6(P^iPr_3)_2$ to give an $OsH_4(P^iPr_3)_2$ species, which coordinates the oxygen atom of the carbonyl group of the ketone and subsequently activates the *ortho*-CH bond of the aromatic group, with the concomitant loss of molecular hydrogen.

2. C−F Activation of Aromatic Ketones. Treatment under reflux of toluene solutions of **1** with 1.2 equiv of pentafluoracetophenone, decafluorobenzophenone, and 2,6-difluoroacetophenone affords after 5 h dark solutions, from which the trihydride complexes $OsH_3\{C_6F_4C(O)R\}(P^iPr_3)_2$ (R = CH_3 (**4**), C_6F_5 (**5**)) and $OsH_3\{C_6H_3FC(O)CH_3\}(P^iPr_3)_2$ (**6**) were isolated in good yield, as a result of the C−F activation of one of the *ortho*-CF bonds of the aromatic ring of the ketones (Scheme 1).

A view of the molecular geometry of **4** is shown in Figure 3. Selected bond distances and angles are listed in Table 1. The coordination geometry around the osmium atom can be rationalized as a distorted pentagonal bipyramid with the two phosphorus atoms of the triisopropylphosphine ligands occupying axial positions (P(1)−Os−P(2) = 162.79(4)°). The osmium sphere is completed by the hydride ligands and the orthometalated ketone, which acts with a bite angle of 75.33(13)°.

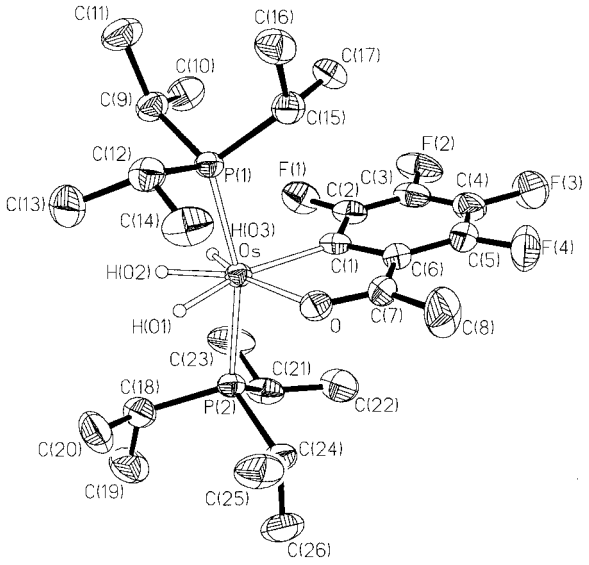

Figure 3. Molecular diagram of the complex $OsH_3\{C_6F_4C(O)CH_3\}(P^iPr_3)_2$ (**4**). Thermal ellipsoids are shown at 50% probability.

Scheme 1

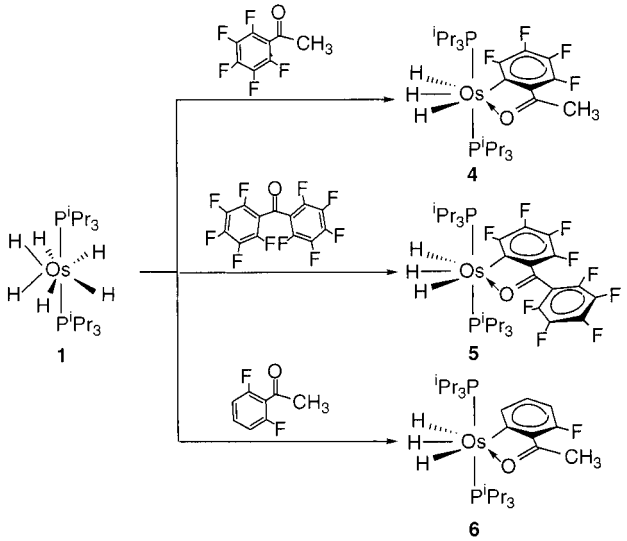

The Os−C(1) bond length of 2.103(4) Å is typical for Os−C(aryl) single bond and agrees well with the values previously found in the complexes $OsH\{C_6H_4\text{-}2\text{-}(E\text{-}CH{=}CHPh)\}(CO)(P^iPr_3)_2$ (2.136(7) Å),[26] $[OsH(\eta^5\text{-}C_5H_5)\{NH{=}C(Ph)C_6H_4\}(P^iPr_3)]BF_4$ (2.10(2) and 2.137(19) Å), $[OsH(\eta^5\text{-}C_5H_5)(PPh_2C_6H_4)(P^iPr_3)]BF_4$ (2.180(9) and 2.136(9) Å),[27] $Os(C_2Ph)\{NH{=}C(Ph)C_6H_4\}(CO)(P^iPr_3)_2$ (2.089(7) Å),[28] $Os(\eta^5\text{-}C_5H_5)\{C_6H_4[C(OH)(Ph)CH{=}CHOC(O)CH_3]\}(P^iPr_3)$ (2.108(11) Å),[29] and $OsCl\{NH{=}C(Ph)C_6H_4\}(\eta^2$-

(25) (a) Esteruelas, M. A.; Lahoz, F. J.; López, A. M.; Oñate, E.; Oro, L. A.; Ruiz, N.; Sola, E.; Tolosa, J. I. *Inorg. Chem.* **1996**, *35*, 7811. (b) Castillo, A.; Esteruelas, M. A.; Oñate, E.; Ruiz, N. *J. Am. Chem. Soc.* **1997**, *119*, 9691. (c) Barea, G.; Esteruelas, M. A.; Lledós, A.; López, A. M.; Oñate, E.; Tolosa, J. I. *Organometallics* **1998**, *17*, 4065. (d) Castillo, A.; Barea, G.; Esteruelas, M. A.; Lahoz, F. J.; Lledós, A.; Maseras, F.; Modrego, J.; Oñate, E.; Oro, L. A.; Ruiz, N.; Sola, E. *Inorg. Chem.* **1999**, *38*, 1814.

(26) Esteruelas, M. A.; Lahoz, F. J.; Oñate, E.; Oro, L. A.; Sola, E *J. Am. Chem. Soc.* **1996**, *118*, 89.

(27) Esteruelas, M. A.; Gutiérrez-Puebla, E.; López, A. M.; Oñate, E.; Tolosa, J. I. *Organometallics* **2000**, *19*, 275.

(28) Esteruelas, M. A.; Lahoz, F. J.; López, A. M.; Oñate, E.; Oro, L. A. *Organometallics* **1995**, *14*, 2496.

Table 1. Selected Bond Distances (Å) and Angles (deg) for the Complex $OsH_3\{C_6F_4C(O)CH_3\}(P^iPr_3)_2$ (4)

Os−P(1)	2.3473(9)	O−C(7)	1.252(5)
Os−P(2)	2.3465(9)	C(1)−C(2)	1.399(5)
Os−O	2.141(3)	C(1)−C(6)	1.433(6)
Os−C(1)	2.103(4)	C(2)−C(3)	1.366(6)
Os−H(01)	1.54(4)	C(3)−C(4)	1.369(7)
Os−H(02)	1.48(5)	C(4)−C(5)	1.369(7)
Os−H(03)	1.56(5)	C(5)−C(6)	1.400(6)
		C(6)−C(7)	1.443(6)
		C(7)−C(8)	1.511(6)
P(1)−Os−P(2)	162.79(4)	H(01)−Os−H(02)	58(2)
P(1)−Os−O	91.89(7)	H(01)−Os−H(03)	114(2)
P(1)−Os−C(1)	96.90(10)	H(02)−Os−H(03)	58(2)
P(1)−Os−H(01)	86.1(15)	Os−O−C(7)	119.1(3)
P(1)−Os−H(02)	81.2(17)	Os−C(1)−C(2)	131.2(2)
P(1)−Os−H(03)	97.3(16)	Os−C(1)−C(6)	114.9(3)
P(2)−Os−O	95.60(7)	O−C(7)−C(6)	116.9(4)
P(2)−Os−C(1)	99.98(10)	O−C(7)−C(8)	118.0(4)
P(2)−Os−H(01)	79.0(15)	C(1)−C(2)−C(3)	124.0(4)
P(2)−Os−H(02)	83.6(17)	C(1)−C(6)−C(5)	121.2(4)
P(2)−Os−H(03)	81.2(16)	C(1)−C(6)−C(7)	113.8(4)
O−Os−C(1)	75.33(13)	C(2)−C(3)−C(4)	121.1(4)
O−Os−H(01)	86.2(16)	C(2)−C(1)−C(6)	113.9(4)
O−Os−H(02)	143.6(19)	C(3)−C(4)−C(5)	118.5(4)
O−Os−H(03)	158.0(16)	C(4)−C(5)−C(6)	121.3(5)
C(1)−Os−H(01)	161.3(16)	C(5)−C(6)−C(7)	125.0(4)
C(1)−Os−H(02)	140.9(19)	C(6)−C(7)−C(8)	125.1(4)
C(1)−Os−H(03)	83.7(16)		

$H_2)(P^iPr_3)_2$ (2.069(4) Å).[25c] The Os−O distance of 2.141(3) Å is that expected for a single bond, whereas the O−C(7) bond length of 1.252(5) Å is similar to that found in free acetophenone (1.217 Å).[30]

In agreement with the structure shown in Figure 3 and with the IR spectra of **2** and **3**, the IR spectra of **4**−**6** in KBr show a ν(CO) vibration between 1600 and 1700 cm^{-1}, along with three bands between 2210 and 1890 cm^{-1}, due to the hydride ligands. In the $^{13}C\{^1H\}$ NMR spectra the resonances corresponding to the metalated carbon atoms are observed between 183 and 215 ppm. The $^{31}P\{^1H\}$ NMR spectra show singlets between 30 and 34 ppm, in accordance with the mutually *trans* position of the phosphine ligands.

The $^{31}P\{^1H\}$ NMR spectra are temperature invariant between 373 and 183 K. However, the ^1H NMR spectra are temperature dependent and consistent with the operation of two thermally activated exchange processes. These exchanges are faster for **4** and **5** than for **6**. At 373 K, the spectra of three compounds show only one broad resonance. Lowering the sample temperature leads to a broadening of the resonance. At 293 K the first decoalescence of **6** occurs, while for **4** and **5**, the first decoalescence is observed at 263 and 233 K, respectively. At 243 K, the second decoalescence of **6** takes place. For **4** and **5**, two broad resonances at −4.11 and −12.23 (**4**) and −3.89 and −11.43 (**5**) ppm, with a 1:2 intensity ratio, are observed even at 183 K. In agreement with the trihydride character of **4**−**6**, T_1(min) values between 86 and 118 ms were found.

As for **2** and **3**, the fastest exchange of the OsH_3 unit of **6** takes place between the central hydride ($\delta = -4.09$) and that situated *cis* to the carbonyl group of the ketone ($\delta = -11.76$). The activation parameters for this exchange are $\Delta H^{\ddagger} = 11.3 \pm 0.2$ kcal·mol^{-1} and $\Delta S^{\ddagger} = 2.5 \pm 0.5$ cal·mol^{-1}·K^{-1}, whereas the activation parameters for the exchange between the central hydride and that situated *cis* to the metalated aromatic ring ($\delta = -13.03$) are $\Delta H^{\ddagger} = 13.9 \pm 0.4$ kcal·mol^{-1} and $\Delta S^{\ddagger} = 3.2 \pm 0.8$ cal·mol^{-1}·K^{-1}. The central hydride and that disposed *cis* to the carbonyl group of the ketone also undergo quantum exchange coupling with a decrease of the H−H coupling constant from 50.5 to 18.9 Hz as the temperature decreases from 223 to 183 K.

Scheme 2

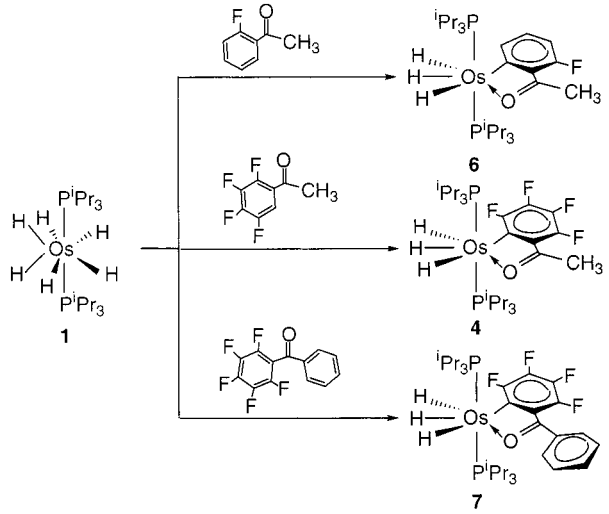

The formation of **4**−**6** could involve a sequence of elemental steps similar to the formation of **2** and **3**, that is, the thermal activation of **1** to give $OsH_4(P^iPr_3)_2$, which coordinates the oxygen atom of the carbonyl group of the ketone, and subsequently activates the *ortho*-CF bond of the aromatic group with the concomitant loss of HF. The activation of the *ortho*-CF bond of fluorinated aromatic ketones suggests that, in the presence of a source of hydrogen, this type of substrate can also be useful for Murai's reaction.

3. C−H Activation versus C−F Activation in Aromatic Ketones. To study the preference for the C−H activation or C−F activation in aromatic ketones, we have also investigated the reactivity of **1** toward partially fluorinated aromatic ketones. The three possible situations in these substrates have been studied (Scheme 2): (i) when the aromatic group contains a fluorine atom in *ortho* position and four hydrogen atoms (2-fluoroacetophenone), (ii) when the aromatic group contains a hydrogen atom in *ortho* position and four fluorine atoms (2,3,4,5-tetrafluoroacetophenone), and (iii) when the ketone contains two aromatic groups, one of them perfluorinated (2,3,4,5,6-pentafluorobenzophenone).

The results shown in Scheme 2 clearly indicate that when the ketone contains only one aromatic ring, the *ortho*-CH activation is preferred over the *ortho*-CF activation. Thus, the treatment under reflux of toluene solutions of **1** with 1.2 equiv of 2-fluoroacetophenone and 2,3,4,5-tetrafluoroacetophenone leads to the C−H activation products, after 5 h, with selectivities of 100%. Complexes **6** and **4** were isolated not only selectively but also in high yield, 80% for **6** and 75% for **4**.

In contrast with the reaction of **1** with 2-fluoroacetophenone and 2,3,4,5-tetrafluoroacetophenone, the treatment under reflux of toluene solutions of **1** with 1.2

(29) Crochet, P.; Esteruelas, M. A.; Gutiérrrez-Puebla, E. *Organometallics* **1998**, *17*, 3141.

(30) 3D Search and Research Using the Cambridge Structural Data Base: Allen, F. H.; Kennard, O. *Chem. Des. Autom. News* **1993**, *8*, 31.

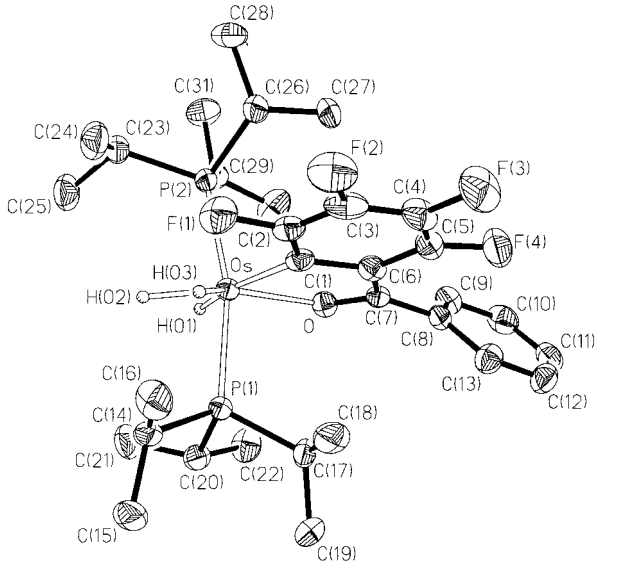

Figure 4. Molecular diagram of the complex $\overline{OsH_3\{C_6F_4C(O)C_6H_5\}}(P^iPr_3)_2$ (**7**). Thermal ellipsoids are shown at 50% probability.

Table 2. Selected Bond Distances (Å) and Angles (deg) for the Complex $\overline{OsH_3\{C_6F_4C(O)C_6H_5\}}(P^iPr_3)_2$ (7)

Os−P(1)	2.3707(13)	O−C(7)	1.269(6)
Os−P(2)	2.3675(13)	C(1)−C(2)	1.406(7)
Os−O	2.158(3)	C(1)−C(6)	1.433(7)
Os−C(1)	2.120(5)	C(2)−C(3)	1.381(8)
Os−H(01)[a]	1.69(3)	C(3)−C(4)	1.393(9)
Os−H(02)[a]	1.68(3)	C(4)−C(5)	1.364(8)
Os−H(03)[a]	1.67(3)	C(5)−C(6)	1.419(8)
		C(6)−C(7)	1.447(7)
		C(7)−C(8)	1.479(7)
P(1)−Os−P(2)	164.65(5)	H(01)[a]−Os−H(02)[a]	65(2)
P(1)−Os−O	90.17(10)	H(01)[a]−Os−H(03)[a]	139(2)
P(1)−Os−C(1)	98.07(14)	H(02)[a]−Os−H(03)[a]	76(2)
P(1)−Os−H(01)[a]	86.9(17)	Os−O−C(7)	119.2(3)
P(1)−Os−H(02)[a]	82.6(17)	Os−C(1)−C(2)	129.1(4)
P(1)−Os−H(03)[a]	75.5(17)	Os−C(1)−C(6)	115.9(4)
P(2)−Os−O	99.85(10)	O−C(7)−C(6)	116.6(4)
P(2)−Os−C(1)	95.81(14)	O−C(7)−C(8)	116.7(5)
P(2)−Os-H(01)[a]	82.4(17)	C(1)−C(2)-C(3)	123.6(5)
P(2)−Os-H(02)[a]	82.8(17)	C(1)−C(6)-C(5)	120.7(5)
P(2)−Os-H(03)[a]	105.5(17)	C(1)−C(6)-C(7)	113.3(5)
O−Os−C(1)	74.58(17)	C(2)−C(3)-C(4)	120.2(5)
O−Os−H(01)[a]	85.0(17)	C(2)−C(1)-C(6)	114.9(5)
O−Os−H(02)[a]	149.0(17)	C(3)−C(4)-C(5)	119.1(5)
O−Os−H(03)[a]	131.4(17)	C(4)−C(5)-C(6)	121.3(5)
C(1)−Os-H(01)[a]	158.9(17)	C(5)−C(6)-C(7)	125.9(5)
C(1)−Os-H(02)[a]	136.2(17)	C(6)−C(7)-C(8)	126.7(5)
C(1)−Os-H(03)[a]	62.3(17)		

[a] For details of hydride refinement in **7** see the Experimental Section.

equiv of 2,3,4,5,6-pentafluorobenzophenone affords the *ortho*-CF activation product, complex $\overline{OsH_3\{C_6F_4C(O)C_6H_5\}}(P^iPr_3)_2$ (**7**), which was selectively isolated in 60% yield.

The *ortho*-CF activation of the perfluorinated ring of the ketone has been confirmed by an X-ray investigation on a monocrystal of **7**. A view of the molecular geometry of this compound is shown in Figure 4. Selected bond distances and angles are listed in Table 2.

The coordination geometry around the osmium atom can be rationalized as a distorted pentagonal bipyramid with the two phosphorus atoms of the triisoprophylphosphine ligands occupying axial positions (P(1)−Os−P(2) = 164.65(5) Å). The osmium sphere is completed by the hydride ligands and the orthometalated ketone, which acts with a bite angle of 74.58(17)°. The Os−C(1) (2.120(5) Å), Os−O (2.158(3) Å), and O−C(7) (1.269(6) Å) bond lengths are similar to those of **4**.

In agreement with the structure shown in Figure 4, the IR spectrum of **7** in KBr shows a ν(CO) band at 1636 cm^{-1} and three ν(Os−H) bands at 1985, 2150, and 2342 cm^{-1}. In the $^{13}C\{^1H\}$ NMR spectrum, the resonance corresponding to the metalated C(1) carbon atom appears at 191.6 ppm as a double multiplet. The $^{31}P\{^1H\}$ NMR spectrum contains a singlet at 32.0 ppm, in accordance with the mutually *trans* disposition of the phosphine ligands. Like the spectra of **2**−**6**, this spectrum is temperature invariant between 373 and 183 K. However the ^1H NMR spectrum is temperature dependent. The behavior of the hydride ligands of the OsH_3 unit of **7** is the same as those of **4** and **5**. At 373 K, the spectrum contains a broad resonance centered at −9.19 ppm. Lowering the sample temperature leads to a broadening of this resonance, which decoalesces at 253 K to give two broad signals centered at −4.39 (1H) and −12.06 (2H) ppm. For these resonances, T_1(min) values of 94 ± 2 and 92 ± 1 ms were found at 228 K.

4. Theoretical Study on the Selectivity of C−H vs C−F Activation. It has been stated in the previous section that the C−H activation is preferred over the

Scheme 3

A) $OsH_4(PH_3)_2$ (**11t**) + $(C_6H_5)COCH_3$ (**8**) ⟶ $\overline{OsH_3\{C_6H_4C(O)CH_3\}}(PH_3)_2$ (**2t**) + H_2 (**0**) **C-H activation**

B) $OsH_4(PH_3)_2$ (**11t**) + $(C_6H_4F)COCH_3$ (**9**) ⟶ $\overline{OsH_3\{C_6H_3FC(O)CH_3\}}(PH_3)_2$ (**6t**) + H_2 (**0**) **C-H activation**

C) $OsH_4(PH_3)_2$ (**11t**) + $(C_6H_4F)COCH_3$ (**9**) ⟶ $\overline{OsH_3\{C_6H_4C(O)CH_3\}}(PH_3)_2$ (**2t**) + HF (**0'**) **C-F activation**

D) $OsH_4(PH_3)_2$ (**11t**) + $(C_6F_5)CO(C_6H_5)$ (**10**) ⟶ $\overline{OsH_3\{C_6H_4C(O)C_6F_5\}}(PH_3)_2$ (**12t**) + H_2 (**0**) **C-H activation**

E) $OsH_4(PH_3)_2$ (**11t**) + $(C_6F_5)CO(C_6H_5)$ (**10**) ⟶ $\overline{OsH_3\{C_6F_4C(O)C_6H_5\}}(PH_3)_2$ (**7t**) + HF (**0'**) **C-F activation**

C−F activation in monoaromatic ketones containing in the aromatic ring both C−H and C−F bonds in the *ortho* position with regard to the carbonyl groups. However, the C−F activation is by no means impossible, as is demonstrated by the set of reactions with fluorinated aromatic compounds. In particular, the reaction of **1** with 2,3,4,5,6-pentafluorobenzophenone emerges as a somewhat surprising example in which the aforementioned selectivity pattern is inverted, and the C−F activation product is obtained despite the presence of C−H bonds in *ortho* positions of one of the aromatic groups of the ketone. To obtain a deeper understanding of the C−H vs C−F activation process, a DFT theoretical study has been carried out for the set of reactions shown is Scheme 3.

In the first stage, only reactants and products have been taken into account. Thus, the reactions of model complex $OsH_6(PH_3)_2$ (**1t**) with $(C_6H_5)COCH_3$ (**8**), (C_6H_4F)-$COCH_3$ (**9**), and $(C_6H_5)CO(C_6F_5)$ (**10**) have been examined in a purely thermodynamic sense. Complex OsH_4-$(PH_3)_2$ (**11t**) is considered as the main reactant and studied in this section, since it is presumed to be the active species. Indeed the calculated value for the thermal activation of **1t** to afford **11t** (15.4 kcal·mol^{-1}) agrees with an easy elimination of H_2 from the hexahydride.

The geometries of reactants have been optimized at the B3LYP level of theory. It is worth mentioning that two structures have been considered for **9**, as the fluorine atom may be *anti* (**9a**) or *syn* (**9b**) with respect to the carbonyl group. Later, it is suggested that this fact could have some influence on the selectivity of C−H vs C−F activation. The obtained structures are depicted in Figure 5 and Figure 6.

Initial complex **1t** has few remarkable features. It is a classical hexahydride without any dihydrogen moiety and adopts a typical dodecahedral coordination geometry, which is in agreement with the neutron diffraction structure previously reported.[31]

The reactive Os(IV) complex (**11t**) can be described as a square pyramidal species with a η^2-H_2 unit (d_{H-H} = 0.931 Å). As expected, the strongest σ-donor hydride occupies the apical position, and the phosphine ligands are essentially *trans* to each other (P−Os−P angle of 170.1°). Thus, we have a 16-electron osmium(II) complex with an empty coordination site available for further coordination of the aryl derivatives.

Two conformations are possible for the aromatic ketone $(C_6H_4F)COCH_3$. An energetical comparison concerning **9a** and **9b** conformations shows that the *syn* arrangement of the *F−C(1)*−C(6)−*C(7)*═*O* unit is unfavorable (**9a** lies 3.7 kcal·mol^{-1} lower than **9b**) because of the repulsive four-electron interactions between F and O in the latter. Moreover, if both structures have a role in the C−H vs C−F bond breaking reaction, the barrier for the rotation that converts **9a** in **9b** must be evaluated. This being a process of rotation around a single bond C(6)−C(7), the barrier that must be surpassed in order to obtain the less favored isomer should not be very high. As a matter of fact, the structure with the

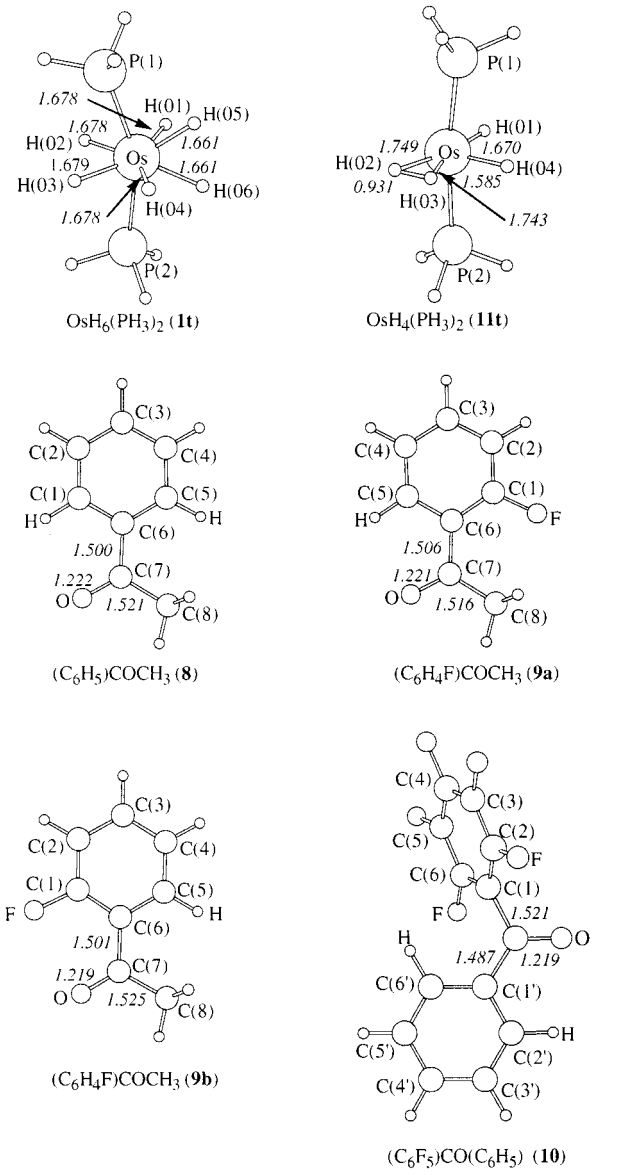

Figure 5. Optimized structures at the B3LYP level of theory for the reactants of the C−H/C−F activation process.

$COCH_3$ group perpendicular to the aryl plane is located 6.6 kcal·mol^{-1} higher than **9a** at the B3LYP level of theory.

Reaction products **2t**, **6t**, **7t**, and **12t** can all be viewed as pentagonal bipyramidal complexes with the phosphine ligands in the axial positions and a slightly distorted arrangement of equatorial ligands. The aryl groups coordinated to the metal lie in the plane perpendicular to P−Os−P axis (the parallel orientation has not been considered mainly for sterical reasons) and coordinate to Os by both C_{ortho} and O, giving rise to a typical five-membered metallacycle. For **7t** the direct comparison with the available X-ray diffraction data shows a good agreement between the experimental and the calculated structure. The largest discrepancy arises from the model simplification of the bulky phosphines of the actual complex, which provokes a stronger bending of the P−Os−P angle in the latter (164.65° vs 171.4°). The geometry of the Os−Aryl unit is nicely reproduced.

(31) Howard, J. A. K.; Johnson, O.; Koetzle T. F.; Spencer, J. L. *Inorg. Chem.* **1987**, *26*, 2930.

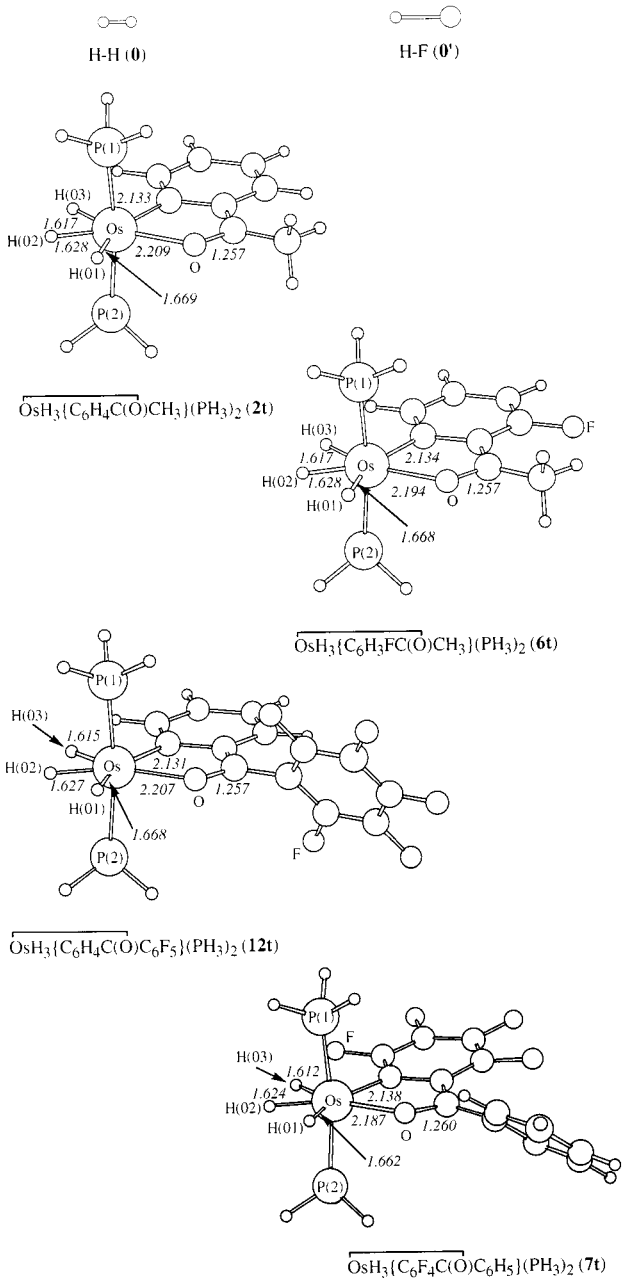

Figure 6. Optimized structures at the B3LYP level of theory for the products of the C−H/C−F activation process.

It must be pointed out that geometries of all these complexes are essentially identical. Although there seems to be a lengthening in the Os−C distances and shortening in the Os−O ones when the ring attached to the metal is fluorinated, the affected geometrical parameters suffer a very mild variation: for instance, Os−C distances differ at maximum by 0.005 Å, whereas the Os−O distance, the most distinct geometrical parameter, ranges from 2.209 Å in **2t** (2.141(3) Å in **4**) to 2.187 Å in **7t** (2.158(3) Å in **7**).

The optimized geometries of reaction products **2t**, **6t**, and **7t** also give an explanation for the different exchange rates observed between pairs of hydrides. It has been stated in previous work that these processes go through dihydrogen states.[25d,32] A facile dihydrogen formation would help lead to a faster exchange rate. For complexes **2t**, **6t**, and **7t**, the metal−hydride bond located *trans* to the carbon atom and *cis* to the carbonyl group is significantly longer than the other two Os−H bonds (1.669 vs 1.628 and 1.617 Å in **2t**, for instance). It comes naturally that a dihydrogen involving this hydride can be reached with a lower energy cost. For this reason, the exchange process in which this hydride has an active role is faster than the exchange process between the other two hydrides.

The calculated energies for the set of reactions A to E is shown in Table 3. It can be stated that both C−H and C−F ruptures are thermodynamically favored. However, C−F activation turns out to be much more exothermic than C−H activation, a result in the line with previous studies.[13] Significantly enough, the preference for the C−F activation product is much more

Table 3. Relative Energies (kcal·mol^{-1}) for the Sets of Reactions A to E Calculated at the B3LYP Level of Theory

reactants	C−H activation	C−F activation
$OsH_4(PH_3)_2$ (**11t**) + $(C_6H_5)COCH_3$ (**8**)	−15.1	
$OsH_4(PH_3)_2$ (**11t**) + $(C_6H_4F)COCH_3$ (**9**)	−15.9	−25.9
$OsH_4(PH_3)_2$ (**11t**) + $(C_6F_5)CO(C_6H_5)$ (**10**)	−15.9	−39.2

Table 4. Crystal Data and Data Collection and Refinement for $OsH_3\{C_6F_4C(O)CH_3\}(P^iPr_3)_2$ (4) and $OsH_3\{C_6F_4C(O)C_6H_5\}(P^iPr_3)_2$ (7)

	4	**7**
	Crystal Data	
formula	$C_{26}H_{48}OF_4OsP_2$	$C_{31}H_{50}OF_4OsP_2$
molecular wt	704.79	766.85
color and habit	red prism	red prism
symmetry, space group	monoclinic, $P2(1)/c$	triclinic, $P\bar{1}$
a, Å	13.199(1)	9.246(1)
b, Å	8.859(1)	11.311(2)
c, Å	25.752(2)	16.336(2)
α, deg	90	76.024(9)
β, deg	99.981(7)	85.905(8)
γ, deg	90	83.839(9)
V, Å^3	2965.6	1646.5
Z	4	2
D_{calc}, g cm^{-3}	1.579	1.547
	Data Collection and Refinement	
diffractometer	Brucker-Siemens P4	
λ(Mo Kα), Å	0.71073	
monochromator	graphite oriented	
μ, mm^{-1}	4.45	4.01
scan type	ω	$\omega/2\theta$
2θ range, deg	$5° \le 2\theta \le 50°$	$5° \le 2\theta \le 50°$
temp, K	173.0(2)	173.0(2)
no.of data collected	6939 (h: −1, 15; k: −1, 10; l: −30, 30)	6077 (h: 0, 10; k: −12, 13; l: −19, 19)
no. of unique data	5185 (merging R factor 0.0336)	5677 (merging R factor 0.0411)
no. of params refined	332	375
R_1[a] [$F^2 > 2\sigma(F^2)$]	0.0239	0.0320
wR_2[b] [all data]	0.0643	0.0870
S[c] [all data]	1.073	0.972

[a] $R_1(F) = \sum||F_o| - |F_c||/\sum|F_o|$. [b] $wR_2(F^2) = \{\sum[w(F_o^2 - F_c^2)^2]/\sum[w(F_o^2)^2]\}^{1/2}$. [c] Goof $= S = \{\sum[w(F_o^2 - F_c^2)^2]/(n - p)\}^{1/2}$, where n is the number of reflections and p is the number of refined parameters.

(32) Maseras, F.; Lledós, A.; Clot, E.; Eisenstein, O. *Chem. Rev.* **2000**, *100*, 601.

marked in the case of reactions D and E, a fact that is undoubtedly related to the exclusive formation of **7t**. A simple way to picture the whole process arises from bonding energy arguments. A balance between broken bonds in the reactants and formed bonds in the products is easily obtained by inspection of reactions B and C (Scheme 3). Assuming that Os−C bonding energy is similar in all cases (this hypothesis seems reasonable taking into account the geometrical similarities between them), the difference between both C−H and C−F activation processes can be traced just taking into account C−F, C−H, H−F, and H−H bond energies. Thus, while the C−F activation process would be disfavored because of the higher energy required to break a C−F bond, this is largely compensated by the greater H−F bond energy compared with the H−H bond energy.

As a consequence of the huge thermodynamic preference found for the C−F activation product, it is obvious that there must be a severe kinetic impediment that makes this reaction unfavorable for 2-fluoroacetophenone and 2,3,4,5-tetrafluoroacetophenone. Two factors may contribute to the inertness of the C−F bond. One of them simply arises from the intrinsic difficulty of the bond-breaking process. Another factor may be derived from the coordinating nature of the aromatic ketone. Assuming that the first step in the activation reaction path is ketone coordination to the metallic center through the oxygen atom (this is in fact a very reasonable hypothesis: Morokuma et al. have demonstrated in their study of the Murai reaction that this kind of reaction goes through such intermediates),[20] it is obvious that this step induces a certain selectivity in the activation process for the reaction of **11t** with **9**, due to the *syn* conformation of the *H−C(5)*−C(6)−*C(7)═O* unit in **9a** and the *syn* conformation of the *F−C(1)*−C(6)−*C(7)═O* unit in **9b**. Thus, if **9a** reacts with **11t**, only a C−H bond is close enough to the metal to be activated, whereas if **9b** reacts instead of **9a** all C−H bonds are too far from the osmium atom. Because **9a** is slightly more favored than **9b**, the time spent in **9a** is longer than that in **9b** and, therefore, the reaction of **11t** with **9a** is more favored than that with **9b**. This might well contribute to the observed pattern. Let us note also that in the reaction of complex **11t** with 2,3,4,5,6-pentafluorobenzophenone we are not faced with this problem, as a slight bending of Os−O axis may face either a C−H or a C−F bond near the osmium. This fact together with the huge thermodynamical preference for **7t** in this particular system may explain why it is possible to shift the reaction toward C−F activation product.

Concluding Remarks

This study has revealed that the hexahydride $OsH_6(P^iPr_3)_2$ can be thermally activated to afford an unsaturated fragment, probably $OsH_2(\eta^2\text{-}H_2)(P^iPr_3)_2$, which is capable of activating *ortho*-CH and *ortho*-CF bonds of aromatic ketones. Thus, the reactions of $OsH_6(P^iPr_3)_2$ with benzophenone and acetophenone lead to $\overline{OsH_3\{C_6H_4C(O)R\}}(P^iPr_3)_2$ (R = Ph, CH_3), and the reactions with pentafluoroacetophenone, decafluorobenzophenone, and 2,6-difluoroacetophenone give $\overline{OsH_3\{C_6F_4C(O)R\}}(P^iPr_3)_2$ (R = CH_3, C_6F_5) and $\overline{OsH_3\{C_6H_3FC(O)CH_3\}}(P^iPr_3)_2$, which are reminiscent of the intermediates proposed by Murai for the *ortho*-alkylation of aromatic ketones.

Complexes $\overline{OsH_3\{C_6H_3FC(O)CH_3\}}(P^iPr_3)_2$ and $\overline{OsH_3\{C_6F_4C(O)CH_3\}}(P^iPr_3)_2$ are also obtained from the reactions of the hexahydride with 2-fluoroacetophenone and 2,3,4,5-tetrafluoroacetophenone, respectively. This indicated that for ketones containing only one aromatic ring, the *ortho*-CH activation is preferred over the *ortho*-CF activation. In contrast, the *ortho*-CF activation is preferred over the *ortho*-CH activation for 2,3,4,5,6-pentafluorobenzophenone. Thus, the reaction of this ketone with $OsH_6(P^iPr_3)_2$ affords $\overline{OsH_3\{C_6F_4C(O)C_6H_5\}}(P^iPr_3)_2$.

In agreement with the CF activation of 2,3,4,5,6-pentafluorobenzophenone theoretical studies suggest that in aromatic ketones the C−F activation is much more favored than the C−H activation, from a thermodynamic point of view. So, the preferred C−H activation in 2-fluoroacethophenone and 2,3,4,5-tetrafluoroacetophenone appears to have kinetic origin, which could be, in part, related with the preferred *anti* arrangement of the *F−C−*C−*C═O* unit of the starting ketones.

In conclusion, complex $OsH_6(P^iPr_3)_2$ activates *ortho*-CH and *ortho*-CF bonds of aromatic ketones. The *ortho*-CH activation is preferred over the *ortho*-CF activation in ketones containing only one aromatic ring, whereas the *ortho*-CF activation is preferred over the *ortho*-CH activation in 2,3,4,5,6-pentafluorobenzophenone.

Experimental Section

Physical Measurements. ^{1}H, ^{19}F, ^{31}P, and ^{13}C{^{1}H} NMR spectra were recorded on either a Varian UNITY 300, Varian Gemini 2000, or a Bruker AXR 300 instrument. The probe temperature of the NMR spectrometers was calibrated at each temperature against a methanol standard. For the T_1 measurements the 180° pulses were calibrated at each temperature. Chemical shifts (expressed in parts per million) are referenced to residual solvent peaks (^{1}H, ^{13}C{^{1}H}), external H_3PO_4 (^{31}P), or external $CFCl_3$ (^{19}F). Coupling constants, J and N ($N = J_{P-H} + J_{P'-H}$ for ^{1}H and $N = J_{P-C} + J_{P'-C}$ for ^{13}C{^{1}H}) are given in hertz. The conventional inversion−recovery method (180−t−90) was used to determine T_1. The Roesy proton experiment was recorded on a Bruker AXR 300 instrument. Infrared spectra were run on a Perkin-Elmer 1730 spectrometer as solids (KBr pellet or Nujol mull). C, H, and N analyses were carried out in a Perkin-Elmer 2400 CHNS/O analyzer. Mass spectra analyses were performed with a VG Autospec instrument. In FAB$^+$ mode ions were produced with the standard Cs^+ gun at ca. 30 kV, and 3-nitrobenzyl alcohol (NBA) was used as the matrix.

Kinetic Analysis. Complete line shape analysis of the ^{1}H-{^{31}P} spectra was achieved using the program gNMR v3.6 for Macintosh (Cherwell Scientific Publishing Limited). The rate constants for various temperatures were obtained by fitting calculated to experimental spectra by full line shape iteractions. We assume $k_{ABC} = k_{BC} = 0$ (A being the central hydride) for all temperatures recorded. At the lowest interval of temperatures the rate for the site exchange process $H_A - H_C$ was fixed to 0 s^{-1}, and the resonance corresponding to the H_C hydride ligand was used to estimate the transverse relaxation time, T_2. The activation parameters $\Delta H^\ddagger$ and $\Delta S^\ddagger$ were calculated by least-squares fit of $\ln(k/T)$ vs $1/T$ (Eyring

equation). Error analysis assumed a 10% error in the rate constant and 1 K in the temperature. Errors were computed by published methods.[33]

Synthesis. All reactions were carried out with rigorous exclusion of air using Schlenk tube techniques. Solvents were dried by known procedures and distilled under argon prior to use. $OsH_6(P^iPr_3)_2$ (**1**) was prepared as reported.[34]

Preparation of $OsH_3\{C_6H_4C(O)C_6H_5\}(P^iPr_3)_2$ (2). A colorless solution of $OsH_6(P^iPr_3)_2$ (100 mg, 0.193 mmol) in 10 mL of toluene was treated with benzophenone (42.20 mg, 0.232 mmol) and heated under reflux for 5 h. The purple solution was filtered through Celite and dried in vacuo. Methanol was added to afford a purple solid, which was washed with methanol at −78 °C and dried in vacuo. Yield: 83.4 mg (62%). Anal. Calcd for $C_{31}H_{54}P_2OOs$: C 53.58; H 7.83. Found: C 53.65; H 7.96. IR (KBr, cm^{-1}): ν(OsH) 2185 (m), 2133 (m), 1946 (s); ν(CO) 1580 (s). ^{1}H NMR (300 MHz, C_6D_6, 293 K): δ 8.94 (d, J(HH) = 7.6 Hz, 1H, H_{Os-Ph}), 8.00 (d, J(HH) = 7.6 Hz, 1H, H_{Os-Ph}), 7.86 (d, J(HH) = 8.1 Hz, 2H, $H_{ortho-Ph}$), 7.18 (dd, J(HH) = 8.1 Hz, J(HH) = 7.5 Hz, 2H, $H_{meta-Ph}$), 7.11 (t, J(HH) = 7.5 Hz, 1H, $H_{para-Ph}$), 6.97 and 6.82 (both vt, J(HH) = 7.6 Hz, 1H, H_{Os-Ph}), 1.83 (m, 6H, PCH), 1.06 (dvt, N = 12.6 Hz, J(HH) = 6.6 Hz, 18H, $PCCH_3$), 1.04 (dvt, N = 12.6 Hz, J(HH) = 6.6 Hz, 18H, $PCCH_3$), −7.92 (br, 2H, OsH), −12.67 (br, 1H, OsH). ^{31}P{^{1}H} NMR (121.42 MHz, C_6D_6, 293 K): δ 31.3 (s). ^{13}C{^{1}H} NMR (75.42 MHz, C_6D_6, 293 K): δ 215.4 (t, J(CP) = 5.6 Hz, OsC), 203.8 (t, J(CP) = 2.3 Hz, C═O), 147.3 (s, CH), 140.8, 139.1 (both s, C_{ipso}), 134.6, 130.4, 130.0, 129.7, 128.4, 118.2 (all s, CH), 27.6 (vt, N = 24.6 Hz, PCH), 20.0 (s, $PCCH_3$), 19.9 (s, $PCCH_3$). MS (FAB$^+$): m/z 692 (M^+ − 2H). $T_{1(min)}$ (ms, OsH_3, 300 MHz, C_7D_8, 228K): 69 ± 6 (−3.35 ppm), 83 ± 3 (−11.13 ppm), 107 ± 1 (−12.23 ppm). $J(H_A-H_B)$ (Hz, C_7D_8): 43.2 (213 K), 37.5 (203 K), 37.5 (193 K), 28.8 (183 K). $J(H_A-H_C) = J(H_B-H_C) = 0$ (Hz, C_7D_8, 213−183 K).

Preparation of $OsH_3\{C_6H_4C(O)CH_3\}(P^iPr_3)_2$ (3). This complex was prepared as described for **2** starting from 100 mg (0.193 mmol) of **1** and acetophenone (27.4 mL, 0.232 mmol). A red solid was obtained. Yield: 74.7 mg (61%). Anal. Calcd for $C_{26}H_{52}P_2OOs$: C 49.35; H 8.28. Found: C 49.20; H 8.28. IR (KBr, cm^{-1}): ν(OsH) 2170 (m), 2149 (m), 1974 (s); ν(CO) 1698 (s). ^{1}H NMR (300 MHz, C_6D_6, 293 K): δ 8.79 (d, J(HH) = 7.5 Hz, 1H, H_{Os-Ph}), 7.56 (d, J(HH) = 7.5 Hz, 1H, H_{Os-Ph}), 6.98 and 6.81 (both vt, J(HH) = 7.5 Hz, 1H, H_{Os-Ph}), 2.46 (t, J(HP) = 1.2 Hz, 3H, CH_3), 1.83 (m, 6H, PCH), 1.04 (dvt, N = 12.6 Hz, J(HH) = 6.9 Hz, 36H, $PCCH_3$), −8.22 (br, 2H, OsH), −13.30 (br, 1H, OsH). ^{31}P{^{1}H} NMR (121.42 MHz, C_6D_6, 293 K): δ 30.4 (s). ^{13}C{^{1}H} NMR (75.42 MHz, C_6D_6, 293 K): δ 211.4 (t, J(CP) = 5.7 Hz, OsC), 207.8 (br s, C═O), 146.8 (s, CH), 142.2 (s, C_{ipso}), 132.0, 130.6, 117.9 (all s, CH), 27.6 (vt, N = 24.4 Hz, PCH), 23.5 (s, CH_3), 20.0 (s, $PCCH_3$), 19.9 (s, $PCCH_3$). MS (FAB$^+$): m/z 630 (M^+ − 2 H). $T_{1(min)}$ (ms, OsH_3, 300 MHz, C_7D_8, 213 K): 99 ± 2 (−4.09 ppm), 100 ± 2 (−12.32 ppm), 111 ± 1 (−13.35 ppm). $J(H_A-H_B)$ (Hz, C_7D_8): 39.0 (213 K), 31.5 (203 K), 28.5 (193 K), 19.5 (183 K). $J(H_A-H_C) = J(H_B-H_C) = 0$ (Hz, C_7D_8, 213−183 K).

Preparation of $OsH_3\{C_6F_4C(O)CH_3\}(P^iPr_3)_2$ (4). This complex was prepared as described for **2** starting from 100 mg (0.193 mmol) of **1** and pentafluoroacetophenone (33.05 mL, 0.232 mmol), *method a;* or 2,3,4,5-tetrafluoroacetophenone (31.69 mL, 0.232 mmol), *method b*. A red solid was obtained. Yield: 101.1 mg (74%), *method a*; 109.0 mg (80%), *method b*. Anal. Calcd for $C_{26}H_{48}F_4P_2OOs$: C 44.31; H 6.86. Found: C 44.02; H 6.95. IR (KBr, cm^{-1}): ν(OsH) 2208 (m), 2140 (m), 2044 (s); ν(CO) 1699 (s). ^{1}H NMR (300 MHz, C_6D_6, 293 K): δ 2.64 (dt, J(HF) = 4.8 Hz, J(HP) = 1.8 Hz, 3H, CH_3), 1.62 (m, 6H, PCH), 0.93 (dvt, N = 13.5 Hz, J(HH) = 6.9 Hz, 18H, $PCCH_3$), 0.90 (dvt, N = 13.5 Hz, J(HH) = 6.9 Hz, 18H, $PCCH_3$), −10.28 (br, 3H, OsH). ^{31}P{^{1}H} NMR (121.42 MHz, C_6D_6, 293 K): δ 30.7 (s). ^{19}F NMR (282.33 MHz, C_6D_6, 293 K): δ −169.7, −152.7, −138.9, and −102.4 (all m, 4F, F_{Os-Ph}). ^{13}C{^{1}H} NMR (75.42 MHz, C_6D_6, 293K): δ 202.9 (s, C═O), 188.3 (dm, $J(CF_{ortho})$ = 56.5 Hz, OsC), 151.4 (ddd, J(CF) = 260.5 Hz, J(CF) = 7.8 Hz, J(CF) = 4 Hz, CF), 148.6 (dd, J(CF) = 226.0 Hz, J(CF) = 4 Hz, CF), 143.2 (ddd, J(CF) = 265.7 Hz, J(CF) = 28.0 Hz, J(CF) = 13.3 Hz, CF), 132.6 (dvt, J(CF) = 241.2 Hz, J(CF) = 16.4 Hz, CF), 124.7 (dd, J(CF) = 15.1 Hz, J(FC) = 4 Hz, C_{ipso}), 28.0 (d, J(CF) = 8.7 Hz, CH_3), 27.6 (vt, N = 24.8 Hz, PCH), 19.7 (s, $PCCH_3$), 19.6 (s, $PCCH_3$). MS (FAB$^+$): m/z 704 (M^+ − 2H). $T_{1(min)}$ (ms, OsH_3, 300 MHz, C_7D_8, 223 K): 111 ± 2 (−4.25 ppm, 1H), 92 ± 1 (−12.82 ppm, 2H).

Preparation of $OsH_3\{C_6F_4C(O)C_6F_5\}(P^iPr_3)_2$ (5). This complex was prepared as described for **2** starting from 100 mg (0.193 mmol) of **1** and decafluorobenzophenone (84.15 mg, 0.232 mmol). A purple solid was obtained. Yield: 93.0 mg (56%). Anal. Calcd for $C_{31}H_{45}F_9P_2OOs$: C 43.46; H 5.29. Found: C 43.35; H 5.32. IR (KBr, cm^{-1}): ν(OsH) 2162 (m), 2023 (m), 1992 (s); ν(CO) 1647 (s). ^{1}H NMR (300 MHz, C_6D_6, 293 K): 1.64 (m, 6H, PCH), 0.99 (dvt, N = 13.5 Hz, J(HH) = 6.9 Hz, 18 H, $PCCH_3$), 0.85 (dvt, N = 13.5 Hz, J(HH) = 6.9 Hz, 18H, $PCCH_3$), −9.01 (br, 3 H, OsH). ^{31}P{^{1}H} NMR (121.42 MHz, C_6D_6, 293 K): δ 34.4 (s). ^{19}F NMR (282.33 MHz, C_6D_6, 293 K): δ −167.9 (m, 1F, F_{Os-Ph}), −162.5 (m, 2F, F_{Ph}), −152.3 (m, 1F, F_{Ph}), −152.0 (m, 1F, F_{Os-Ph}), −143.3 (m, 2F, F_{Ph}), −140.2 (m, 1F, F_{Os-Ph}), −102.3 (m, 1F, F_{Os-Ph}). ^{13}C{^{1}H} NMR (75.42 MHz, C_6D_6, 293 K): δ 198.1 (dm, $J(CF_{ortho})$ = 61.7 Hz, OsC), 181.7 (s, C═O), 150−110 (multiplets due to 9 aromatic carbon atoms), 27.0 (vt, N = 25.7 Hz, PCH), 19.6 (s, $PCCH_3$), 19.2 (s, $PCCH_3$). MS (FAB$^+$): m/z 856 (M^+ − 2H). $T_{1(min)}$ (ms, OsH_3, 300 MHz, C_7D_8, 223 K): 87 ± 7 (−3.89 ppm, 1H), 93 ± 2 (−11.43 ppm, 2H).

Preparation of $OsH_3\{C_6H_3FC(O)CH_3\}(P^iPr_3)_2$ (6). This complex was prepared as described for **2** starting from 100 mg (0.193 mmol) of **1** and 2-fluoroacetophenone (28.6 mL, 0.232 mmol), *method a*; or 2,6-difluoroacetophenone (33.0 mL, 0.232 mmol), *method b*.A red solid was obtained. Yield: 90.9 mg (72%), *method a*; 94.4 mg (75%), *method b*. Anal. Calcd for $C_{26}H_{51}FP_2OOs$: C 47.98; H 7.90. Found: C 47.74; H 8.16. IR (KBr, cm^{-1}): ν(OsH) 2161 (m), 1968 (m), 1890 (s); ν(CO) 1601 (s). ^{1}H NMR (300 MHz, C_6D_6, 293 K): δ 8.48 (d, J(HH) = 7.5 Hz, 1H, H_{Os-Ph}), 6.74 (vtd, J(HH) = 7.5 Hz, J(HF) = 5.1 Hz, 1H, H_{Os-Ph}), 6.42 (dd, J(HH) = 7.5 Hz, J (HF) = 12.3 Hz, 1H, H_{Os-Ph}), 2.86 (dt, J(HF) = 4.8 Hz, J(HP) = 1.5 Hz, 3H, CH_3), 1.76 (m, 6H, PCH), 1.02 (dvt, N = 12.9 Hz, J(HH) = 6.6 Hz, 36H, $PCCH_3$), −8.34 (br, 2H, OsH), −13.27 (br, 1H, OsH). ^{31}P-{^{1}H} NMR (121.42 MHz, C_6D_6, 293 K): δ 30.3 (s). ^{19}F NMR (282.33 MHz, C_6D_6, 293 K): δ −111.2 (m). ^{13}C{^{1}H} NMR (75.42 MHz, C_6D_6, 293 K): δ 215.8 (dt, J(CP) = 5.8 Hz, J(CF) = 5.7 Hz, OsC), 205.2 (dt, J(CF) = 5.5 Hz, J(CP) = 2.7 Hz, C═O), 168.4 (d, J(CF) = 260.6 Hz, CF), 142.6 (d, J(CF) = 5 Hz), 131.6 (d, J(CF) = 7.8 Hz, CF), 130.6 (d, J(CF) = 5.0 Hz, C_{ipso}), 103.4 (d, J(CF) = 21.6 Hz, C−F), 28.6 (d, J(CF) = 8.7 Hz, CH_3), 27.6 (vt, N = 24.4 Hz, PCH), 19.9 (s, $PCCH_3$), 19.8 (s, $PCCH_3$). MS (FAB$^+$): m/z = 650 (M^+ − 2 H). $T_{1(min)}$ (ms, OsH_3, 300 MHz, C_7D_8, 213 K): 84 ± 3 (−4.09 ppm), 103 ± 2 (−11.76 ppm), 118 ± 1 (−13.03 ppm). $J(H_A-H_B)$ (Hz, C_7D_8): 50.5 (223 K), 44.2 (213 K), 37.9 (203 K), 31.6 (193 K), 18.9 (183 K). $J(H_A-H_C) = J(H_B-H_C) = 0$ (Hz, C_7D_8, 223−183 K).

Preparation of $OsH_3\{C_6F_4C(O)C_6H_5\}(P^iPr_3)_2$ (7). This complex was prepared as described for **2** starting from 100 mg (0.193 mmol) of **1** and 2,3,4,5,6-pentafluorobenzophenone (63.23 mg, 0.232 mmol). A purple solid was obtained. Yield: 89.0 mg (60%). Anal. Calcd for $C_{31}H_{50}F_4P_2OOs$: C 48.55; H 6.57. Found: C 48.15; H 6.57. IR (KBr, cm^{-1}): ν(OsH) 2342 (m), 2150 (m), 1985 (s); ν(CO) 1636 (s). ^{1}H NMR (300 MHz,

(33) Morse, P. M.; Spencer, M. D.; Wilson, S. R.; Girolami, G. S. *Organometallics* **1994**, *13*, 1646.
(34) Aracama, M.; Esteruelas, M. A.; Lahoz, F. J.; López, J. A.; Meyer, U.; Oro, L. A.; Werner, H. *Inorg. Chem*. **1991**, *30*, 288.

C_6D_6, 293 K): δ 7.66 (dd, J(HH) = 6.8 Hz, J(FH) = 5.4 Hz, 2 H, H_{Ph}), 7.12 (vt, J(HH) = 6.8 Hz, 2H, H_{Ph}), 7.07 (t, J(HH) = 6.8 Hz, 1H, H_{Ph}), 1.82 (m, 6H, PCH), 1.14 (dvt, N = 12.9 Hz, J(HH) = 6.9 Hz, 36H, PCCH_3), −9.19 (br, 3H, OsH). $^{31}P\{^1H\}$ NMR (121.42 MHz, C_6D_6, 293 K): δ 32.0 (s). ^{19}F NMR (282.33 MHz, C_6D_6, 293 K): δ −169.3 (m, 1F, F_{Os-Ph}), −153.7 (m, 1F, F_{Os-Ph}), −132.4 (m, 1F, F_{Os-Ph}), −102.5 (m, 1F, F_{Os-Ph}). $^{13}C\{^1H\}$ NMR (75.42 MHz, C_6D_6, 293 K): δ 199.3 (s, C═O), 191.6 (dm, J(CF_{ortho}) = 56.8 Hz, OsC), 150.9 (ddd, J(CF) = 261.2 Hz, J(CF) = 10.3 Hz, J(CF) = 3.1 Hz, CF), 148.6 (dm, J(CF) = 225.5 Hz, CF), 143.1 (ddd, J(CF) = 264.8 Hz, J(CF) = 28.3 Hz, J(CF) = 12.8 Hz. CF), 140.4 (s, CH), 128.9 (s, CH), 128.8 (s, CH), 127.9 (s, C_{ipso}), 123.9 (dm, J(CF) = 20.2 Hz, $C_{ipso-Os-Ph}$), 27.7 (vt, N = 25.3 Hz, P*C*H), 19.8 (s, PC*C*H_3), 19.7 (s, PC*C*H_3). MS (FAB$^+$): m/z 766 (M^+ − 2 H). $T_{1(min)}$ (ms, OsH_3, 300 MHz, C_7D_8, 228 K): 94 ± 2 (−4.14 ppm, 1H), 92 ± 1 (−11.70 ppm, 2H).

Crystal Data for 4 and 7. Crystals suitable for X-ray diffraction analysis were mounted onto a glass fiber and transferred to an Bruker-Siemens-P4 (**4** and **7**, T = 173.0(2) K) automatic diffractometer (Mo Kα radiation, graphite monocromator, λ = 0.71073 Å). Accurate unit cell parameters were determined by least-squares fitting from the settings of high-angle reflections. Data were collected by the ω(**4**)$\omega/2\theta$(**7**) scan method. Lorentz and polarization corrections were applied. Decay was monitored by measuring three standards throughout data collection. Corrections for decay and absorption (semiempirical ψ-scan method) were also applied.

The structures were solved by Patterson methods and refined by full-matrix least-squares on F^2 (**4** and **7**).[35] Non hydrogen atoms were anisotropically refined, and the hydrogen atoms were observed or included at idealized positions. For **4**, the three hydride ligands were observed in the difference Fourier maps and refined as free isotropic atoms. For **7**, we can also observe three peaks with appropriate intensity and geometry for the hydride ligands. However, they do not support a refinement as free isotropic atoms because of the presence of residual electronic density close to the hydride ligands (particularly H(03)). For this reason, we refine this ligands with the distance to the osmium atom and isotropic parameters restrained to the same values.

Computational Details. All calculations were carried out with the Gaussian 98 package of programs[36] using the density functional theory (DFT)[37] with the B3LYP functional.[38] An effective core potential operator was used to replace the 60 innermost electrons of Os.[39] The basis set for the metal was that associated with the pseudopotential,[39] with a standard valence double-ζ LANL2DZ contraction.[36] The basis set for the hydrogen atoms directly attached to the metal, as well as for the H atoms involved in the bond-breaking process, was a double-ζ supplemented with a polarization p shell.[40a,b] A 6-31G-(d) basis was used for all the ring C atoms[40c] except for **7t**, **10**, and **12** model compounds, in which only the *ipso* and *ortho* C atoms were treated with such accuracy, the rest of the ring carbons being described with a 6-31G basis set.[40a] The carbonyl C atom was also described with a 6-31G(d) basis set, as well as the O atom and the F atom at the *ortho* position of the ring.[40c] The rest of the atoms were described with a 6-31G basis set.[40a,b]

Acknowledgment. Financial support from the DGES of Spain (Projects PB98-0916-02-01 and PB98-1591, Programa de Promoción General de Conocimiento) is acknowledged. J.T. acknowledges the "Direcció General de Recerca de la Generalitat de Catalunya" for a grant. R.C. and P.B. thank the "Ministerio de Ciencia y Tecnología" for their respective grants. The use of computational facilities of the Centre de Supercomputació i Comunicacions de Catalunya is gratefully appreciated as well.

Supporting Information Available: Tables of positional and displacement parameters, crystallographic data, and bond lengths and angles. This material is available free of charge via the Internet at http://pubs.acs.org.

OM000844R

(35) Sheldrick, G. M. *SHELX-97*; Göttingen, 1997.

(36) Frisch, M. J.; Trucks, G. W.; Schlegel, H. B.; Scuseria, G. E.; Robb, M. A.; Cheeseman, J. R.; Zakrzewski, V. G.; Montgomery, J. A., Jr.; Stratmann, R. E.; Burant, J. C.; Dapprich, S.; Millam, J. M.; Daniels, A. D.; Kudin, K. N.; Strain, M. C.; Farkas, O.; Tomasi, J.; Barone, V.; Cossi, M.; Cammi, R.; Mennucci, B.; Pomelli, C.; Adamo, C.; Clifford, S.; Ochterski, J.; Petersson, G. A.; Ayala, P. Y.; Cui, Q.; Morokuma, K.; Malick, D. K.; Rabuck, A. D.; Raghavachari, K.; Foresman, J. B.; Cioslowski, J.; Ortiz, J. V.; Stefanov, B. B.; Liu, G.; Liashenko, A.; Piskorz, P.; Komaromi, I.; Gomperts, R.; Martin, R. L.; Fox, D. J.; Keith, T.; Al-Laham, M. A.; Peng, C. Y.; Nanayakkara, A.; Gonzalez, C.; Challacombe, M.; Gill, P. M. W.; Johnson, B.; Chen, W.; Wong, M. W.; Andres, J. L.; Gonzalez, C.; Head-Gordon, M.; Replogle, E. S.; Pople, J. A. *Gaussian 98, Revision A.6*; Gaussian, Inc.: Pittsburgh, PA, 1998.

(37) (a) Parr, R. G.; Yang, W. *Density Functional Theory of Atoms and Molecules*; Oxford University Press: Oxford, U.K., 1989. (b) Ziegler, T. *Chem. Rev.* **1991**, *91*, 651.

(38) (a) Lee, C.; Yang, W.; Parr, R. G. *Phys. Rev. B* **1988**, *37*, 785. (b) Becke, A. D. *J. Chem. Phys.* **1993**, *98*, 5648. (c) Stephens, P. J.; Devlin, F. J.; Chabalowski, C. F.; Frisch, M. J. *J. Phys. Chem.* **1994**, *98*, 11623.

(39) Hay, P. J.; Wadt, W. R. *J. Chem. Phys.* **1985**, *82*, 299.

(40) (a) Hehre, W. J.; Ditchfield, R.; Pople, J. A. *J. Chem. Phys.* **1972**, *56*, 2257. (b) Hariharan, P. C.; Pople, J. A. *Theor. Chim. Acta* **1973**, *28*, 213. (c) Francl, M. M.; Pietro, W. J.; Hehre, W. J.; Binkley, J. S.; Gordon, M. S.; DeFrees, D. J.; Pople, J. A. *J. Chem. Phys.* **1982**, *77*, 3654.